AD-A086 335 WASHINGTON UNIV SEATTLE DEPT OF MECHANICAL ENGINEERING F/G 20/11
INFLUENCE OF SMALL SCALE YIELDING ON DYNAMIC FRACTURE.(U)
MAY 80 A S KOBAYASHI, M RAMULU, B S KANG N00014-76-C-0060
UNCLASSIFIED TR-38 NL

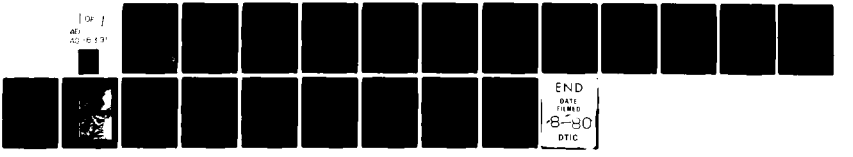

END
DATE FILMED
8-80
DTIC

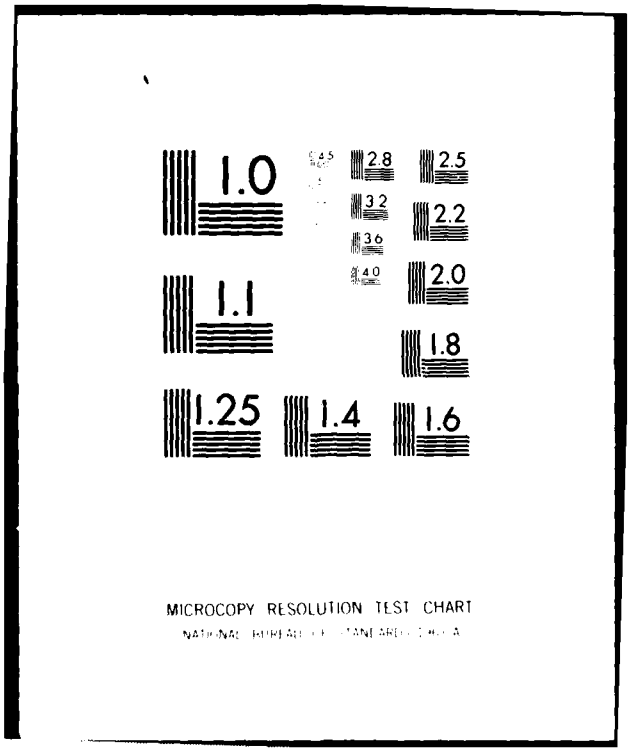
1.0
1.1
1.25
1.4
1.6
1.8
2.0
2.2
2.5
2.8
3.2
3.6
4.0
4.5
MICROCOPY RESOLUTION TEST CHART

LEVEL II (12)



Office of Naval Research

Contract N00014-76-0060 NR 064-478

Technical Report No. 38

# INFLUENCE OF SMALL-SCALE YIELDING ON DYNAMIC FRACTURE

by

A.S. Kobayashi, M. Ramulu, and B.S.-J Kang

May 1980



The research reported in this technical report was made possible through support extended to the Department of Mechanical Engineering, University of Washington, by the Office of Naval Research under Contract N00014-76-C-0060 NR 064-478.




Department of Mechanical Engineering

College of Engineering

University of Washington

SUMMARY

Dynamic fracture and crack-arrest responses of the well-discussed wedge-loaded rectangular, double cantilever beam (WL-RDCB) specimens machined from a 3.2 mm thick annealed polycarbonate sheet were studied by dynamic photoelasticity and dynamic finite element analysis. A small, but finite plastic yield zone surrounded the propagating crack which resulted in crack velocities, dynamic fracture toughness and crack arrest toughness lower than those observed previously in 6.4 mm thick polycarbonate fracture specimens.

## INTRODUCTION

Current experimental and numerical investigations in dynamic fracture involve extensive use of dynamic photoelasticity [1,2] dynamic caustics [3], dynamic finite difference analysis [4,5], and dynamic finite element analysis [6,7]. The results published in the above are based on the theory of elasto-dynamics and have evoked a controversy regarding the existence of a material property, i.e., a unique dynamic fracture toughness, $K_{ID}$, versus crack velocity relation, $\dot{a}$, as a material property which governs dynamic crack propagation and arrest [1,2,6,8]. Despite this unresolved controversy on elastodynamic fracture, the increasing research efforts in this field should eventually lead to a phenomenological dynamic fracture criterion which can be used in either finite difference or finite element codes to predict crack propagation histories in actual structures. For example, recent numerical simulation of dynamic fracture in a thermally shocked structure [9] correlated well with experimental results [10] and undoubtedly such practical applications will increase as the controversies in elastodynamic fracture are resolved.

Unlike the efforts in elastodynamic fracture, little basic research in dynamic ductile fracture, particularly in the presence of large scale yielding has been conducted to date. Earlier investigations on dynamic ductile fracture, including

those of Kanninen et al [11], Hahn et al [12] and Ogasawara et al [13] as well as the recent papers by Koshiga et al [14] and Nora et al [15] involved phenomenological modelings of specific experimental observations. While these results are useful in predicting dynamic ductile fracture responses in specific structures, they fail to address the basic laws governing dynamic ductile fracture.

One major difficulty in dynamic ductile fracture research is the lack of suitable experimental technique with which the dynamic states of stress, strains, plastic yield zone, etc. can be measured directly for detailed scrutiny. In contrast, dynamic photoelasticity and dynamic caustics provide optical imaging from which the dynamic stress intensity, $K_I^{dyn}$ , among others can be extracted for elastodynamic fracture studies. Lacking a pure experimental approach, one method which can be used is the combined experimental-numerical procedure for computing dynamic fracture parameters. In this procedure, experimental results such as crack position versus time in a fracturing specimen, is used to drive a crack in a finite element model of the fracture specimen. The numerical results, such as the equivalent dynamic stress intensity factor for elastic analysis, dynamic J-integral and crack opening angle, COA, among others can then be studied as candidate dynamic ductile fracture criteria. The soundness of this procedure when used in elastic analysis has been verified by one of the authors [2,16]. It was then used in a series of sensitivity studies on the influence of various dynamic fracture toughness, $K_{ID}$, versus crack velocity, $\dot{a}$, relations [17,18]. An obvious extension of this elastic procedure is its use in elasto-plastic analysis.

This paper reports some preliminary results obtained in the course of developing an experimental-numerical procedure for determining dynamic ductile fracture toughness which could be used to characterize the dynamic ductile fracture.

## EXPERIMENTAL ANALYSIS

The concurrent experimental analysis in this investigation consisted of

dynamic photoelasticity using thin, i.e., 3.2 mm thick, polycarbonate wedge-loaded, rectangular double cantilever beam (WL-RCB) specimens which is shown by Figure 1. The annealed polycarbonate, from which the specimens were machined, has a well-defined yield point of 44 MPa, flows under high stresses, and exhibits tensile instability with accompanying Lueder's bands. Under high strain rate loading, such as in the vicinity of a propagating crack tip, the strain-rate sensitive polycarbonate fractures in a cleavage mode without the large plastic zone ahead of the propagating crack tip. Such ductile to brittle transition in dynamic loading of polycarbonate is discussed in Reference [19]. Despite this cleavage fracture appearance, the dynamic photoelastic patterns in Figure 2(a) and 2(b) show that the propagating crack tip is preceded by a small yield zone of 1.2 mm and 0.4 mm diameters, respectively, and thus, represent dynamic fracture in the presence of small scale yielding. The elastic region surrounding this small yield zone also provides the elasto-dynamic state which can be used to extract apparent elastic fracture parameter for characterizing such dynamic ductile fracture. For example, the isochromatics form the standard loops from which apparent dynamic stress intensity factor can be extracted through the use of well-known elasto-dynamic near-field solutions [20]. Possible errors involved in characterizing the elasto-plastic dynamic field with such straight forward application of elastic analysis will be discussed later. The 16-spark gap Cranz-Shardin camera and the associated dynamic photoelastic systems used to record 16 discrete dynamic photoelastic patterns in the fracturing polycarbonate WL-RDCB specimen has been described in many previous papers and thus will not be repeated here.

In the as-received condition, the polycarbonate sheet exhibits considerable residual stress distribution and thus the sheets were annealed after rough cutting. This annealing, which caused some distortion and shrinkage, consisted of overnight heating at 160°C, followed by gradual cooling at the rate of 5°C per hour. The starter crack consisted of 0.4 mm wide edge crack approximately 25 mm length which

was machined and then chiseled to simulate a somewhat blunt crack tip. Static and dynamic stress-fringe constant and Poisson's ratio at various strain rates, all of which were determined previously [21], were used in data reductions. Static modulus of elasticity of E = 2.00 GPa and the yield strength of 44 MPa were determined separately for this particular polycarbonate sheet.

## CRACK TIP ISOCHROMATICS IN THE PRESENCE OF SMALL SCALE YIELDING

The influence of small scale yielding on the dynamic isochromatics surrounding the crack tip was studied by a static Dugdale strip yield model (DM) as shown in Figure 3. Since the Westergaard's stress function for a partially pressurized semi-infinite crack tip is known [22], the crack tip isochromatics, $\tau_m$, for a stationary crack with a Dugdale strip yield of length $r_y$, can be expressed as

$$\tau_m = \frac{1}{2}[(\sigma_{xx} - \sigma_{yy})^2 + 4\tau_{xy}^2]^{\frac{1}{2}} \tag{1a}$$

where

$$\sigma_{xx} - \sigma_{yy} = K_I \frac{\sin\theta_{DM}}{\sqrt{2\pi r_{DM}}} \frac{\frac{r_y}{r_{DM}} \sin\frac{\theta_{DM}}{2} + \sin\frac{3\theta_{DM}}{2}}{(\frac{b}{r})^2 + 1 + 2\frac{r_y}{r_{DM}}\cos\theta_{DM}} \tag{1b}$$

$$2\tau_{xy} = -K_I \frac{\sin\theta_{DM}}{2\pi r_{DM}} \frac{\frac{r_y}{r_{DM}} \cos\frac{\theta_{DM}}{2} + \cos\frac{3\theta_{DM}}{2}}{(\frac{r_y}{r_{DM}})^2 + 1 + 2\frac{r_y}{r_{DM}}\cos\theta_{DM}} \tag{1c}$$

where $r_{DM}$ and $\theta_{DM}$ are the polar coordinates with origin at the DM crack tip in Figure 3. The stress intensity factor, $K_I$, corresponds to the negative of the stress intensity factor at the DM crack tip without the Dugdale strip yield zone. From the equality, the length of the DM zone becomes

$$r_y = \frac{\pi}{8} \left( \frac{K_I}{\sigma_y} \right)^2 \qquad (2)$$

where $\sigma_y$ is the yield strength of the material.

The resultant crack tip isochromatics in the presence of a DM zone can be obtained numerically for the highly loaded crack tip at the onset of crack propagation. For estimated stress intensity factor of $K_I$ = 2.44 MPa$\sqrt{m}$, yield strength of $\sigma_y$ = 44 MPa and an isochromatic frange order of 7-1/2 or $\tau_{max}$ = 84.8 MPa in the 3.2 mm WL-RDCB specimen. The DM strip yield length is $r_y$ = 1.3 mm. Figure 4 shows the estimated crack tip isochromatics with the DM zone and the experimentally observed isochromatics of Figure 2(a). The significant difference between the estimated and experimental isochromatics indicate the amount of plasticity correction necessary to increase the elastic $K_I$ in the presence of small scale yielding.

The procedure then for estimating the apparent stress intensity factor from the isochromatics in the presence of small scale yielding is to first estimate the location of the far end of the crack tip yield zone or the DM crack tip location in the photoelastic pattern. An overdeterministic least square method [23] is then used to fit at the DM crack tip a two parameter, elastic crack tip stress field to the experimentally recorded isochromatics. Using the elastic stress intensity factor thus computed, the DM strip yield length $r_y$ is determined by equation (2) and the estimated isochromatics is reconstructed numerically by the use of equation (1). Should the computed $r_y$ be substantially different from the measured $r_y$, then $r_y$ must be remeasured and the above numerical procedure is repeated. Fortunately, such repeated measurement was not necessary in the test analyzed for this paper. The ratio of the maximum radial distances, $r_M$ and $r_{DM}$ in Figure 4, is the plasticity correction factor. This procedure must be repeated until the succeeding plasticity correction factor approaches unity. However, in view of the

approximate nature of the entire procedure, this iteration procedure was not programmed into this data reduction scheme.

The above procedure is based on static crack tip yielding and obviously must be modified for dynamic analysis. It, however, provides a first order estimate of the plasticity correction involved in deducing the apparent dynamic stress intensity factor from the dynamic isochromatics in the presence of small scale yielding.

## DYNAMIC FINITE ELEMENT ANALYSIS

The dynamic finite element algorithm used in this study differs with that presented two years ago [24]. The new fracture package [2] includes a mechanism for gradual release in crack tip nodal force as well as an iteration routine to assure agreement between the prescribed and computed crack tip nodal forces in this explicit code. Figure 1 shows the finite element breakdown used in this plane stress analysis which is considered more appropriate for these thin fracture specimens, despite the cleavage fracture surfaces. The dynamic finite element code was executed in its elastic-plastic mode. The coarseness of finite element breakdown, i.e., 3.2 mm square in comparison to the observed maximum plastic yield zone of 1 mm, however, forced the actual computation into its elastic mode except for the initial 1-2 microseconds in crack propagation time. As a result, the dynamic stress intensity factor, $K_I^{dyn}$ , was computed elastically using the dissipated energy at the released node with Freund's equation [25].

## RESULTS OF DYNAMIC PHOTOELASTICITY

A total of seven dynamic photoelastic tests were conducted. Figure 2 shows two typical dynamic photoelastic patterns of a fracturing polycarbonate WL-RDCB specimen. These dynamic photoelastic patterns show crack tip shadow patterns which are believed to be caustics [3] generated by the large plastic strains in the con-

fined plastic region ahead of the propagating crack tip. The size of such a plastic zone ranges from $r_y$ = 1.3 mm to 0.04 mm. Minor distortions of the otherwise elastic isochromatics in the vicinity of this plastic region is also noted.

Apparent dynamic stress intensity factor, $K_I^{dyn}$ , was computed by using the data reduction procedure described previously. Figure 5 shows the apparent dynamic fracture toughness, which were obtained by this procedure, during dynamic fracture and crack arrest in a polycarbonate WL-DCB specimen. The general variation of these experimental results differs slightly with those obtained by others [3,7]. The apparent dynamic fracture toughness continues to decrease in the former while distinct regions of contant $K_{ID}$ after crack propagation were observed in the latter. The crack initiation stress intensity factor of $K_{IQ}$ = 7.37 MPa$\sqrt{m}$ is more than twice of the pop-in fracture toughness of $K_{IC}$ = 3.4 MPa$\sqrt{m}$ measured previously [21]. The measured apparent crack arrest fracture toughness of $K_{Ia}$ = 1.0 MPa m, however, is considerably lower than this pop-in fracture toughness and lower than the $K_{Ia}$ = 1.4 MPa$\sqrt{m}$ reported for the 6.4 mm polycarbonate fracture specimens [2].

Also shown in Figure 5 is the crack velocity change with crack extension in this WL-RDCB specimen. This crack velocity history was duplicated in the other six specimens and are similar in shape to those reported by others [3,26] but the terminal velocity is lower than that in Reference [2].

## RESULTS OF DYNAMIC FINITE ELEMENT ANALYSIS

Figure 5 shows the calculated dynamic stress intensity factor obtained through elasto-dynamic finite element analysis. As mentioned previously, the finite element analysis was executed in its elastic-plastic mode, but elastic analysis prevailed except for the initial 1-2 microseconds of crack propagation. Agreements between calculated dynamic stress intensity factors and the measured

dynamic fracture toughness during crack propagation history are apparent. The precipitous drop in calculated dynamic stress intensity factor at the initial phase of crack propagation can be in part attributed to the infinite plate syndrome discussed by Perl [27]. It was also found that this precipitous drop in dynamic stress intensity factor could be moderated by assigning a gradually increasing crack velocity during the first 30-50 microseconds of crack propagation following Reference [27]. Recent experimental results [20,28,29], however, show that the crack velocity of a blunt starter crack immediately reaches the terminal velocity upon propagation and does not gradually approach the terminal velosity as postulated in Reference [27] during this crucial initial period of crack propagation. These experimental evidences thus precluded adjustments of crack velocity to reduce the precipitous drop in $K_I^{dyn}$ .

Figure 6 shows the energy partitions during crack propagation in the WL-RDCB specimens discussed previously. Although the dissipated plastic energy at the plastic yield zone was not computed in this coarse finite element model, the decreasing total energy in Figure 6 indicated qualitatively, the small plastic energy dissipated in the fracture process of polycarbonate WL-RDCB specimen.

## CONCLUSIONS

1. Small-scale yielding at the propagating crack tip does change the shape of the crack-tip dynamic isochromatics.
2. Crack velocity, dynamic fracture toughness and crack arrest toughness are lower in the presence of small-scale yielding at the propagating crack tip.
3. Dynamic stress intensity factor obtained by elasto-dynamic finite element analysis are in good agreement with the apparent dynamic fracture toughness obtained through an elasto-plastic data reduction of the dynamic isochromatics in the presence of small scale yielding. Elasto-plastic dynamic finite element analysis, does not appear necessary for such dynamic fracture problems.

4. The decreasing total energy indicate the influence of dissipated plastic energy in the presence of a small plastic zone.

ACKNOWLEDGEMENTS

The results of this investigation were obtained in a research contract funded by the Office of Naval Research under Contract No. N0014-76-C-0600 NR 064-478. The authors wish to acknowledge the support and encouragement of Dr. N. Perrone of ONR during the course of this investigation.

REFERENCES

1. DALLY, J.W., "Dynamic Photoelastic Studies of Fracture," Experimental Mechanics, No. 1, 19, No. 10, pp. 349-367, October 1979.

2. KOBAYASHI, A.S., SEO, K., JOU, J.Y. and URABE, U., "A Dynamic Analyses of Modified Compact-Tension Specimens Using Homalite-100 and Polycarbonate Plates," Experimental Mechanics, Vol. 20, No. 3, pp. 73-79, March 1980.

3. KALTHOFF, J.F., BEINERT, J. and WINKLER, S., "Measurements of Dynamic Stress Intensity Factors for Fast Running and Arresting Cracks in Double-Cantilever-Beam Specimen," Fast Fracture and Crack Arrest, ASTM STP 627, pp. 161-176, July 1977.

4. SCHMUELY, M., and PERL, M., "The SMF2D Code for Proper Simulation of Crack Propagation," to be published in Crack Arrest Methodology and Applications, ASTM STP.

5. POPELAR, C.H. and GEHLEN, P.C., "Modeling of Dynamic Crack Propagation II Validation of Two-Dimensional Analysis," International Journal of Fracture, Vol. 15, pp. 159-178, 1979.

6. KOBAYASHI, A.S., "Dynamic Fracture Analysis by Dynamic Finite Element Method-Generation and Propagation Analysis," Nonlinear and Dynamic Fracture Mechanics, edited by N. Perrone and S.N. Atluri, ASME, pp. 19-36, 1979.

7. ATLURI, S.N., NISHIOKA, T. and NAKAGAKI, M., "Numerical Modeling of Dynamic and Nonlinear Crack Propagation in Finite Bodies, by Moving Singularities," ibid loc cit, ppl 37-66.

8. KANNINEN, M.F., GEHLEN, P.C., BARNES, C.P., HOAGLAND, R.G., HAHN, G.T. and POPELAR, C.H., "Dynamic Crack Propagation Under Impact Loading," ibid loc cit, pp. 195-200.

9. HAHN, G.T., HOAGLAND, R.G., GEHLEN, R.C. and ROSENFIELD, A.R., "Analysis of Crack Arrest in Reactor Pressure Vessel," ASME Paper No. 78-MAT-16.

10. CHEVERTON, R.D. and ISKANDER, S.K., "Application of Static and Dynamic Crack Arrest Theory to Thermal Shock Experiment TSE-4," NUREG/CR-0767, ORNL/NUREG-57, June 1979.

11. KANNINEN, M.F., MUKHERJEE, A.K., ROSENFIELD, A.R. and HAHN, G.T., "The Speed of Ductile-Crack Propagation and the Dynamics of Flaw in Metals," Mechanical Behavior of Materials Under Dynamic Loads (ed. by U.S. Lindholm), Springer-Verlag, pp. 96, 1968.

12. HAHN, G.T., SARATE, M., KANNINEN, M.F. and ROSENFIELD, A.R., "A Model for Unstable Shear Crack Propagation in Pipes Containing Gas Pressures," International Journal of Fracture, Vol. 9, pp. 209-222, June 1973.

13. OGASAWARA, M., MIMURA, M., and ISHIGURO, K., "Laboratory Test for Unstable Ductile Fracture," Proceedings of International Symposium on Crack Propagation in Pipelines, Newcastel-Upon-Tyne, March 1974.

14. KOSHIGA, F., KURITA, Y., AKIYAMA, T. and KAWAHARA, M., "Shear Fracture Propagation by DCB Testing," ASME Journal of Pressure Vessel Technology, Vol. 100, pp. 18-23, February 1980.

15. NORA, Y., FUKUDA, M., NOGAKI, N., KOGA, T. and TAKEUCHI, I., "Study on Resisting of Various Types of Steels Against Propagating Shear Fracture by Modified West Jefferson Type Burst Test," ASME Preprint 78-PVP-71, 1980.

16. KOBAYASHI, A.S., "Experimental-Numerical Analysis of a Running Crack," Recent Research on Mechanical Behavior of Solids, University of Tokyo Press, pp. 291-313, 1979.

17. HODULAK, L., KOBAYASHI, A.S., EMERY, A.F., "Influence of Dynamic Fracture Toughness on Dynamic Crack Propagation," to be published in Engineering Fracture Mechanics.

18. HODULAK, L., KOBAYASHI, A.S., EMERY, A.F., "A Critical Examination of a Numerical Fracture Dynamic Code," to be published in Fracture Mechanics (12th) ASTM STP.

19. YEE, A.F., "The Yield and Deformation Behavior of Some Polycarbonate Blend," General Electric Technical Information Series, 76 CRD 130, August 1976.

20. KOBAYASHI, A.S., and MALL, S., "Dynamic Fracture Toughness of Homalite-100." Experimental Mechanics, Vol. 18, No. 1, pp. 11-18, January 1978.

21. MALL, S., and KOBAYASHI, A.S., "Dynamic Photoelastic and Dynamic Finite Element Analyses of Polycarbonate Dynamic Tear Specimens," Fracture Mechanics, edited by C.W. Smith, ASTM STP 677, pp. 498-510, 1979.

22. TADA, H., PARIS, P.C. and IRWIN, G.R., The Stress Analysis of Cracks Handbook, Del Research Corporation, Hellertown, PA, p. 37, 1973.

23. KOBAYASHI, A.S. and RAMULU, M., "Dynamic Stress Intensity Factors for Unsymmetric Dynamic Isochromatics," to be published in Experimental Mechanics.

24. KOBAYASHI, A.S., MALL, S., URABE, Y. and EMERY, A.F., "A Numerical Dynamic Fracture Analysis of Three-Wedge-Loaded DCB Specimens," Proceeding of the International Conference on Numerical Analysis in Fracture Mechanics, University College of Swansea, pp. 673-684, January 9-13, 1978.

25. FREUND, L.B., "Crack Propagation in an Elastic Solid Subjected to General Loading I, Constant Rate of Extension," Journal of Mechanics and Physics of Solids, Vol. 20, pp. 129-140, 1972.

26. KOBAYASHI, T., DALLY, J.W. and FOURNEY, W.L., "Influence of Specimen Geometry on Crack Propagation and Arrest Behavior," Proceedings of the 6th International Conference on Experimental Stress Analysis, Munchen, 1978.

27. PERL, M., "An Improved Dynamic Analysis of an Initiating and Fast-Running Griffith Crack in a Finite Rectangular plate," this conference proceeding.

28. MALL, S., KOBAYASHI, A.S. and URABE, Y., "Dynamic Photoelastic and Dynamic Finite-Element Analyses of Dynamic-Tear-Test Specimens," Experimental Mechanics, Vol. 18, No. 12, pp. 449-456, December 1978.

29. DALLY, J.W. and SHUKLA, A., "Dynamic Crack Behavior at Initiation," Mechanics Research Communication, Vol. 6 (4), pp. 239-244, 1979.

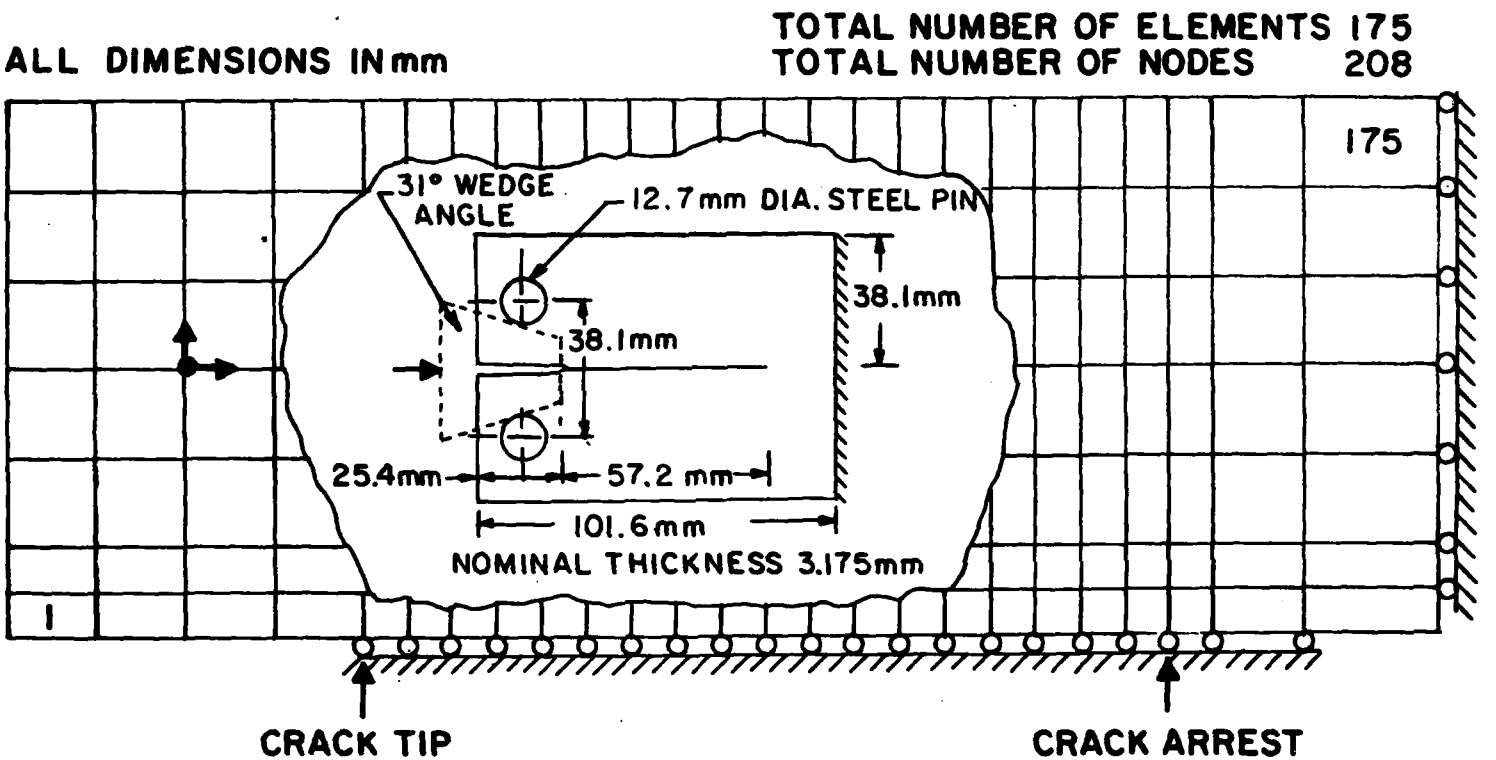


FIGURE 1. FINITE ELEMENT BREAKDOWN OF WL-DCB SPECIMEN.

(a) 1ST FRAME 7 $\mu$ SECONDS

(b) 7TH FRAME 71 $\mu$ SECONDS

FIGURE 2. TYPICAL DYNAMIC PHOTOELASTIC PATTERNS IN POLYCARBONATE WL-DCB SPECIMEN NO. K031380-P.

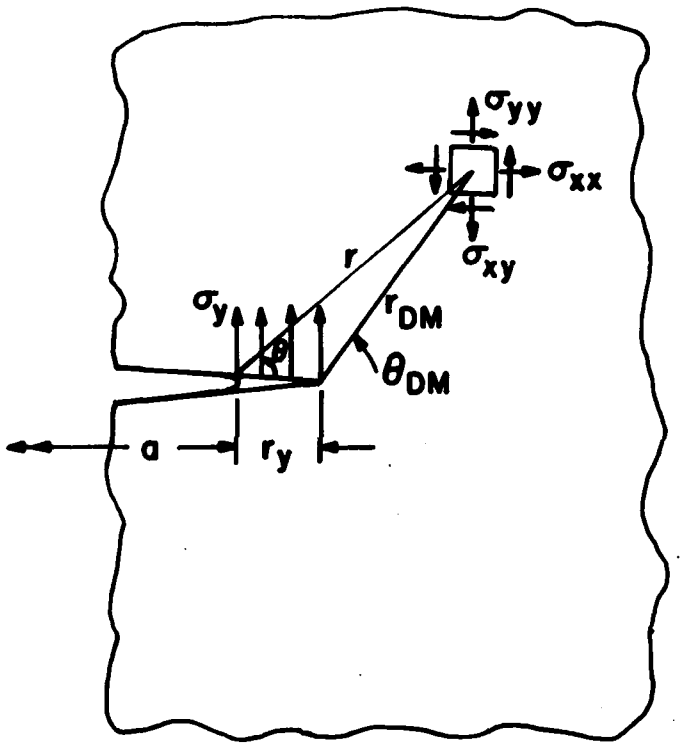


FIGURE 3. DUGDALE STRIP YIELD ZONE AT THE CRACK TIP OF A SEMI-INFINITE CRACK.

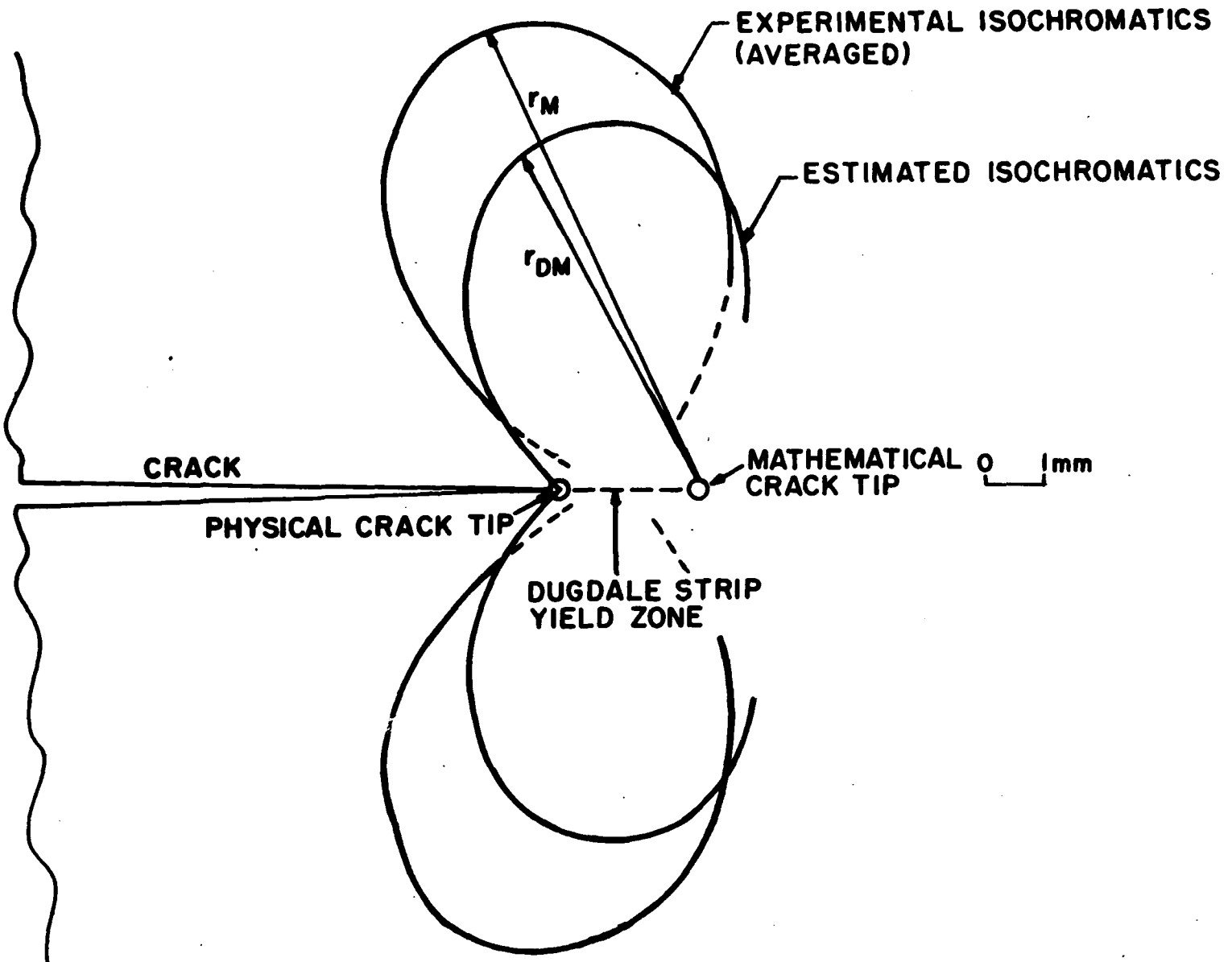


FIGURE 4. EXPERIMENTAL AND ESTIMATED ISOCHROMATICS.

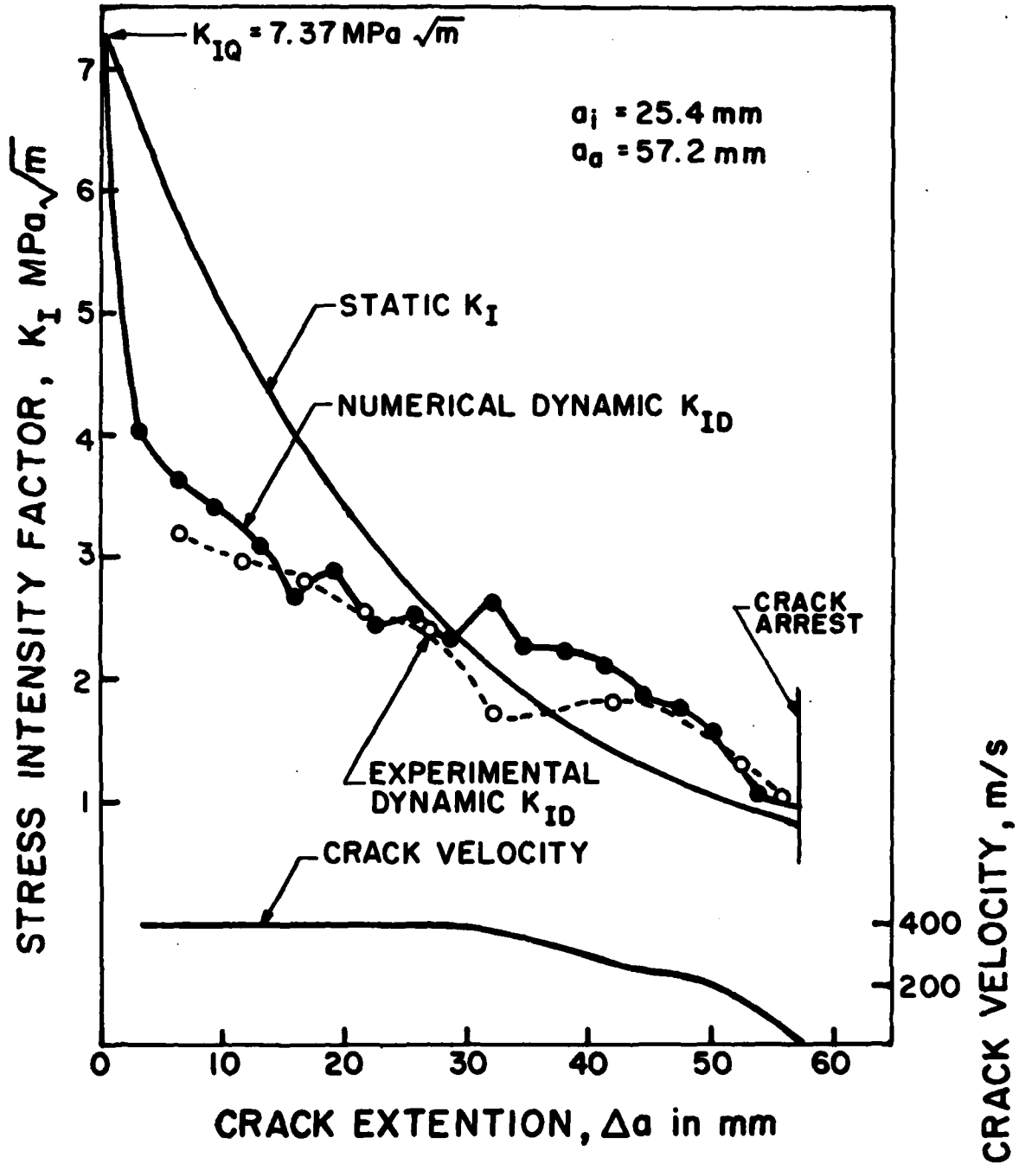


FIGURE 5. STRESS INTENSITY FACTORS OF A FRACTURING POLYCARBONATE WL-DCB SPECIMEN NO. KO31380-P.

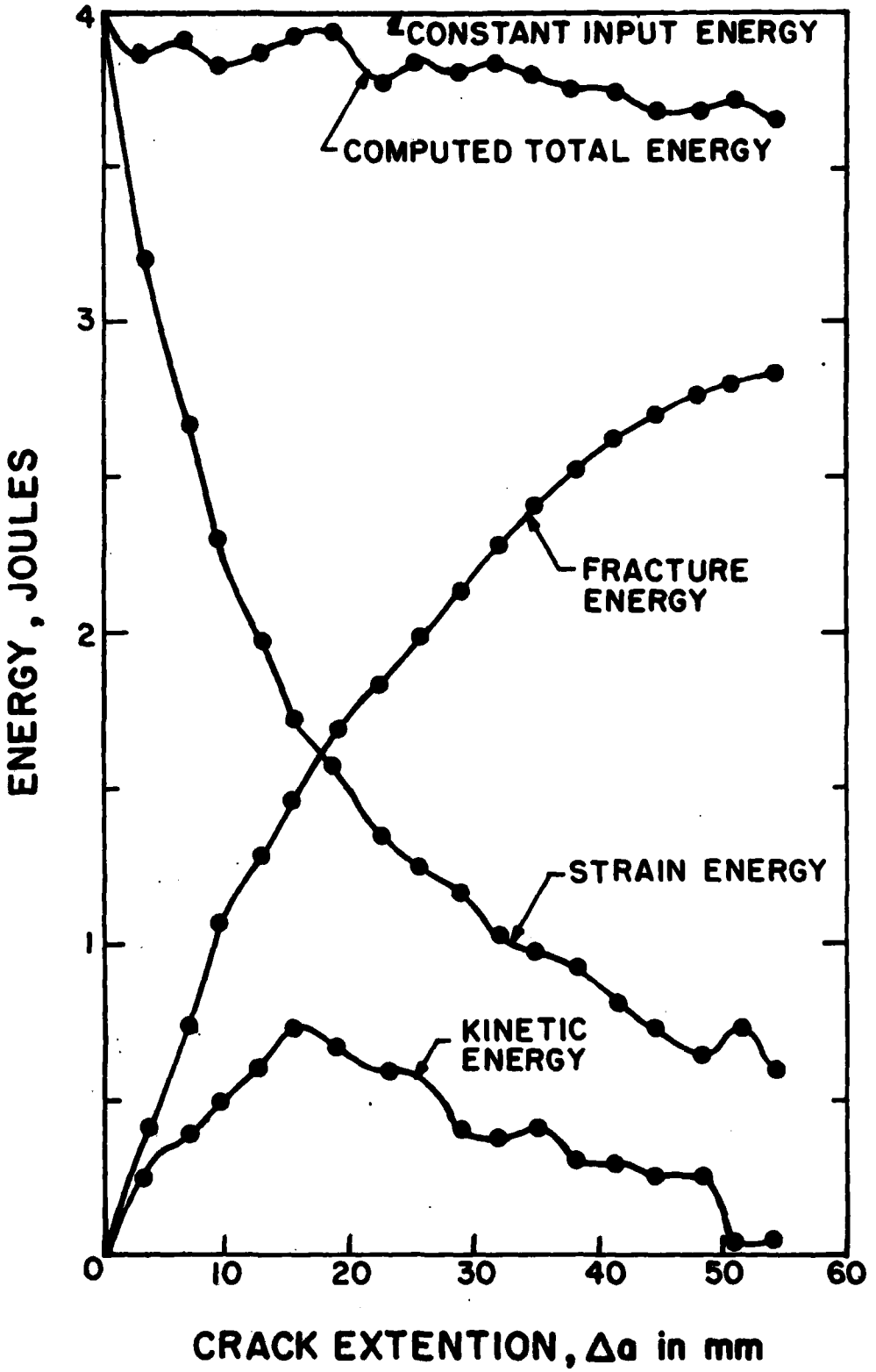


FIGURE 6. ENERGY OF A FRACTURING POLYCARBONATE WL-DCB SPECIMEN NO.K031380-P.

Part 1 - Government
Administrative and Liaison Activities

Office of Naval Research
Department of the Navy
Arlington, Virginia 22217
Attn: Code 474 (2)
Code 471
Code 200

Director
Office of Naval Research
Branch Office
666 Summer Street
Boston, Massachusetts 02210

Director
Office of Naval Research
Branch Office
536 South Clark Street
Chicago, Illinois 60605

Director
Office of Naval Research
New York Area Office
715 Broadway - 5th Floor
New York, New York 10003

Director
Office of Naval Research
Branch Office
1030 East Green Street
Pasadena, California 91106

Naval Research Laboratory (6)
Code 2627
Washington, D.C. 20375

Defense Documentation Center (12)
Cameron Station
Alexandria, Virginia 22314

Navy

Underwater Explosion Research Division
Naval Ship Research and Development
Center
Norfolk Naval Shipyard
Portsmouth, Virginia 23709
Attn: Dr. E. Palmer, Code 177

Navy (Con't.)

Naval Research Laboratory
Washington, D.C. 20375
Attn: Code 8400
8410
8430
8440
6300
6390
6380

David W. Taylor Naval Ship Research
and Development Center
Annapolis, Maryland 21402
Attn: Code 2740
28
281

Naval Weapons Center
China Lake, California 93555
Attn: Code 4062
4520

Commanding Officer
Naval Civil Engineering Laboratory
Code L31
Port Hueneme, California 93041

Naval Surface Weapons Center
White Oak
Silver Spring, Maryland 20910
Attn: Code R-10
G-402
K-82

Technical Director
Naval Ocean Systems Center
San Diego, California 92152

Supervisor of Shipbuilding
U.S. Navy
Newport News, Virginia 23607

Navy Underwater Sound
Reference Division
Naval Research Laboratory
P.O. Box 8337
Orlando, Florida 32806

Navy (Con't.)

Chief of Naval Operations
Department of the Navy
Washington, D.C. 20350
Attn: Code OP-098

Strategic Systems Project Office
Department of the Navy
Washington, D.C. 20376
Attn: NSP-200

Naval Air Systems Command
Department of the Navy
Washington, D.C. 20361
Attn: Code 5302 (Aerospace and Structures)
604 (Technical Library)
3208 (Structures)

Naval Air Development Center
Warminster, Pennsylvania 18974
Attn: Aerospace Mechanics
Code 606

U.S. Naval Academy
Engineering Department
Annapolis, Maryland 21402

Naval Facilities Engineering Command
200 Stovall Street
Alexandria, Virginia 22332
Attn: Code 03 (Research and Development)
048
045
14114 (Technical Library)

Naval Sea Systems Command
Department of the Navy
Washington, D.C. 20362
Attn: Code 05H
312
322
323
05R
32R

Navy (Con't.)

Commander and Director
David W. Taylor Naval Ship
Research and Development Center
Bethesda, Maryland 20084
Attn: Code 042
17
172
173
174
1800
1844
012.2
1900
1901
1945
1960
1962

Naval Underwater Systems Center
Newport, Rhode Island 02840
Attn: Dr. R. Trainor

Naval Surface Weapons Center
Dahlgren Laboratory
Dahlgren, Virginia 22448
Attn: Code G04
G30

Technical Director
Mare Island Naval Shipyard
Vallejo, California 94592

U.S. Naval Postgraduate School
Library
Code 0384
Monterey, California 93940

Webb Institute of Naval Architecture
Attn: Librarian
Crescent Beach Road, Glen Cove
Long Island, New York 11542

Army

Commanding Officer (2)
U.S. Army Research Office
P.O. Box 12211
Research Triangle Park, NC 27709
Attn: Mr. J. J. Murray, CRD-AA-IP



Army (Con't.)

Watervliet Arsenal
MAGGS Research Center
Watervliet, New York 12189
Attn: Director of Research

U.S. Army Materials and Mechanics
Research Center
Watertown, Massachusetts 02172
Attn: Dr. R. Shea, DRXMR-T

U.S. Army Missile Research and
Development Center
Redstone Scientific Information
Center
Chief, Document Section
Redstone Arsenal, Alabama 35809

Army Research and Development
Center
Fort Belvoir, Virginia 22060

NASA

National Aeronautics and Space
Administration
Structures Research Division
Langley Research Center
Langley Station
Hampton, Virginia 23365

National Aeronautics and Space
Administration
Associate Administrator for Advanced
Research and Technology
Washington, D.C. 20546

Air Force

Wright-Patterson Air Force Base
Dayton, Ohio 45433
Attn: AFFDL (FB)
(FBE)
(FBS)
(FBR)
ASD (ENFDE)

Air Force (Con't.)

Chief Applied Mechanics Group
U.S. Air Force Institute of Technology
Wright-Patterson Air Force Base
Dayton, Ohio 45433

Chief, Civil Engineering Branch
WLRC, Research Division
Air Force Weapons Laboratory
Kirtland Air Force Base
Albuquerque, New Mexico 87117

Air Force Office of Scientific Researc
Bolling Air Force Base
Washington, D.C. 20332
Attn: Mechanics Division

Department of the Air Force
Air University Library
Maxwell Air Force Base
Montgomery, Alabama 36112

Other Government Activities

Commandant
Chief, Testing and Development Divisic
U.S. Coast Guard
1300 E Street, NW.
Washington, D.C. 20226

Technical Director
Marine Corps Development
and Education Command
Quantico, Virginia 22134

Director Defense Research
and Engineering
Technical Library
Room 3C128
The Pentagon
Washington, D.C. 20301



Other Government Activities (Con't)

Dr. M. Gaus
National Science Foundation
Environmental Research Division
Washington, D.C. 20550

Library of Congress
Science and Technology Division
Washington, D.C. 20540

Director
Defense Nuclear Agency
Washington, D.C. 20305
Attn: SPSS

Mr. Jerome Persh
Staff Specialist for Materials
and Structures
OUSDR&E, The Pentagon
Room 3D1089
Washington, D.C. 20301

Chief, Airframe and Equipment Branch
FS-120
Office of Flight Standards
Federal Aviation Agency
Washington, D.C. 20553

National Academy of Sciences
National Research Council
Ship Hull Research Committee
2101 Constitution Avenue
Washington, D.C. 20418
Attn: Mr. A. R. Lytle

National Science Foundation
Engineering Mechanics Section
Division of Engineering
Washington, D.C. 20550

Picatinny Arsenal
Plastics Technical Evaluation Center
Attn: Technical Information Section
Dover, New Jersey 07801

Maritime Administration
Office of Maritime Technology
14th and Constitution Avenue, NW.
Washington, D.C. 20230

PART 2 - Contractors and Other Technical Collaborators

Universities

Dr. J. Tinsley Oden
University of Texas at Austin
345 Engineering Science Building
Austin, Texas 78712

Professor Julius Miklowitz
California Institute of Technology
Division of Engineering
and Applied Sciences
Pasadena, California 91109

Dr. Harold Liebowitz, Dean
School of Engineering and
Applied Science
George Washington University
Washington, D.C. 20052

Professor Eli Sternberg
California Institute of Technology
Division of Engineering and
Applied Sciences
Pasadena, California 91109

Professor Paul M. Naghdi
University of California
Department of Mechanical Engineering
Berkeley, California 94720

Professor A. J. Durelli
Oakland University
School of Engineering
Rochester, Missouri 48063

Professor P. L. DiMaggio
Columbia University
Department of Civil Engineering
New York, New York 10027

Professor Norman Jones
The University of Liverpool
Department of Mechanical Engineering
P. O. Box 147
Brownlow Hill
Liverpool L69 3BX
England

Professor E. J. Skudrzyk
Pennsylvania State University
Applied Research Laboratory
Department of Physics
State College, Pennsylvania 16801

Universities (Con't.)

Professor J. Klosner
Polytechnic Institute of New York
Department of Mechanical and
Aerospace Engineering
333 Jay Street
Brooklyn, New York 11201

Professor R. A. Schapery
Texas A&M University
Department of Civil Engineering
College Station, Texas 77843

Professor Walter D. Pilkey
University of Virginia
Research Laboratories for the
Engineering Sciences and
Applied Sciences
Charlottesville, Virginia 22901

Professor K. D. Willmert
Clarkson College of Technology
Department of Mechanical Engineering
Potsdam, New York 13676

Dr. Walter E. Haisler
Texas A&M University
Aerospace Engineering Department
College Station, Texas 77843

Dr. Hussein A. Kamal
University of Arizona
Department of Aerospace and
Mechanical Engineering
Tucson, Arizona 85721

Dr. S. J. Fenves
Carnegie-Mellon University
Department of Civil Engineering
Schenley Park
Pittsburgh, Pennsylvania 15213

Dr. Ronald L. Huston
Department of Engineering Analysis
University of Cincinnati
Cincinnati, Ohio 45221

474:MP:716:lab
78u474-619

Universities (Con't)

Professor G. C. M. Sih
Lehigh University
Institute of Fracture and
Solid Mechanics
Bethlehem, Pennsylvania 18015

Professor Albert S. Kobayashi
University of Washington
Department of Mechanical Engineering
Seattle, Washington 98105

Professor Daniel Frederick
Virginia Polytechnic Institute and
State University
Department of Engineering Mechanics
Blacksburg, Virginia 24061

Professor A. C. Eringen
Princeton University
Department of Aerospace and
Mechanical Sciences
Princeton, New Jersey 08540

Professor E. H. Lee
Stanford University
Division of Engineering Mechanics
Stanford, California 94305

Professor Albert I. King
Wayne State University
Biomechanics Research Center
Detroit, Michigan 48202

Dr. V. R. Hodgson
Wayne State University
School of Medicine
Detroit, Michigan 48202

Dean B. A. Boley
Northwestern University
Department of Civil Engineering
Evanston, Illinois 60201

474:MP:716:lab
78u474-619

Universities (Con't)

Professor P. G. Hodge, Jr.
University of Minnesota
Department of Aerospace Engineering
and Mechanics
Minneapolis, Minnesota 55455

Dr. D. C. Drucker
University of Illinois
Dean of Engineering
Urbana, Illinois 61801

Professor N. M. Newmark
University of Illinois
Department of Civil Engineering
Urbana, Illinois 61803

Professor E. Reissner
University of California, San Diego
Department of Applied Mechanics
La Jolla, California 92037

Professor William A. Nash
University of Massachusetts
Department of Mechanics and
Aerospace Engineering
Amherst, Massachusetts 01002

Professor G. Herrmann
Stanford University
Department of Applied Mechanics
Stanford, California 94305

Professor J. D. Achenbach
Northwest University
Department of Civil Engineering
Evanston, Illinois 60201

Professor S. B. Dong
University of California
Department of Mechanics
Los Angeles, California 90024

Professor Bert Paul
University of Pennsylvania
Towne School of Civil and
Mechanical Engineering
Philadelphia, Pennsylvania 19104

474:MP:716:lab
78u474-619

Universities (Con't)

Professor H. W. Liu
Syracuse University
Department of Chemical Engineering
and Metallurgy
Syracuse, New York 13210

Professor S. Bodner
Technion R&D Foundation
Haifa, Israel

Professor Werner Goldsmith
University of California
Department of Mechanical Engineering
Berkeley, California 94720

Professor R. S. Rivlin
Lehigh University
Center for the Application
of Mathematics
Bethlehem, Pennsylvania 18015

Professor F. A. Cozzarelli
State University of New York at
Buffalo
Division of Interdisciplinary Studies
Karr Parker Engineering Building
Chemistry Road
Buffalo, New York 14214

Professor Joseph L. Rose
Drexel University
Department of Mechanical Engineering
and Mechanics
Philadelphia, Pennsylvania 19104

Professor B. K. Donaldson
University of Maryland
Aerospace Engineering Department
College Park, Maryland 20742

Professor Joseph A. Clark
Catholic University of America
Department of Mechanical Engineering
Washington, D.C. 20064

474:MP:716:lab
78u474-619

Universities (Con't)

Dr. Samuel B. Batdorf
University of California
School of Engineering
and Applied Science
Los Angeles, California 90024

Professor Isaac Fried
Boston University
Department of Mathematics
Boston, Massachusetts 02215

Professor E. Krempl
Rensselaer Polytechnic Institute
Division of Engineering
Engineering Mechanics
Troy, New York 12181

Dr. Jack R. Vinson
University of Delaware
Department of Mechanical and Aerospace
Engineering and the Center for
Composite Materials
Newark, Delaware 19711

Dr. J. Duffy
Brown University
Division of Engineering
Providence, Rhode Island 02912

Dr. J. L. Swedlow
Carnegie-Mellon University
Department of Mechanical Engineering
Pittsburgh, Pennsylvania 15213

Dr. V. K. Varadan
Ohio State University Research Foundation
Department of Engineering Mechanics
Columbus, Ohio 43210

Dr. I. Khalil
University of Pennsylvania
Department of Metallurgy and
Materials Science
College of Engineering and
Applied Science
Philadelphia, Pennsylvania 19104

474:MP:716:lab
78u474-619

Universities (Con't)

Dr. Jackson C. S. Yang
University of Maryland
Department of Mechanical Engineering
College Park, Maryland 20742

Professor T. Y. Chang
University of Akron
Department of Civil Engineering
Akron, Ohio 44325

Professor Charles W. Bert
University of Oklahoma
School of Aerospace, Mechanical,
and Nuclear Engineering
Norman, Oklahoma 73019

Professor Satya N. Atluri
Georgia Institute of Technology
School of Engineering and
Mechanics
Atlanta, Georgia 30332

Professor Graham F. Carey
University of Texas at Austin
Department of Aerospace Engineering
and Engineering Mechanics
Austin, Texas 78712

Dr. S. S. Wang
University of Illinois
Department of Theoretical and
Applied Mechanics
Urbana, Illinois 61801

Industry and Research Institutes

Dr. Herman Hobbs
Kaman AviDyne
Division of Kaman
Sciences Corporation
Burlington, Massachusetts 01803

Argonne National Laboratory
Library Services Department
9700 South Cass Avenue
Argonne, Illinois 60440

474:MP:716:lab
78u474-619

Industry and Research Institutes (Con't)

Dr. M. C. Junger
Cambridge Acoustical Associates
54 Rindge Avenue Extension
Cambridge, Massachusetts 02140

Dr. V. Godino
General Dynamics Corporation
Electric Boat Division
Groton, Connecticut 06340

Dr. J. E. Greenspon
J. G. Engineering Research Associates
3831 Menlo Drive
Baltimore, Maryland 21215

Newport News Shipbuilding and
Dry Dock Company
Library
Newport News, Virginia 23607

Dr. W. F. Bozich
McDonnell Douglas Corporation
3301 Bolsa Avenue
Huntington Beach, California 92647

Dr. H. H. Abramson
Southwest Research Institute
8500 Culebra Road
San Antonio, Texas 78284

Dr. R. C. DeHart
Southwest Research Institute
8500 Culebra Road
San Antonio, Texas 78284

Dr. M. L. Baron
Weidlinger Associates
110 East 59th Street
New York, New York 10022

Dr. T. L. Geers
Lockheed Missiles and Space Company
3251 Hanover Street
Palo Alto, California 94304

Mr. William Caywood
Applied Physics Laboratory
Johns Hopkins Road
Laurel, Maryland 20810

474:MP:716:lab
78u474-619

Industry and Research Institutes (Con't)

Dr. Robert E. Dunham
Pacifica Technology
P.O. Box 148
Del Mar, California 92014

Dr. M. F. Kanninen
Battelle Columbus Laboratories
505 King Avenue
Columbus, Ohio 43201

Dr. A. A. Wochrain
Daedalean Associates, Inc.
Springlake Research Road
15110 Frederick Road
Woodbine, Maryland 21797

Dr. James W. Jones
Swanson Service Corporation
P.O. Box 5413
Huntington Beach, California 92646

Dr. Robert E. Nickell
Applied Science and Technology
3344 North Torrey Pines Court
Suite 220
La Jolla, California 92037

Dr. Kevin Thomas
Westinghouse Electric Corp.
Advanced Reactors Division
P. O. Box 158
Madison, Pennsylvania 15663

UNCLASSIFIED

SECURITY CLASSIFICATION OF THIS PAGE (When Data Entered)

| REPORT DOCUMENTATION PAGE | READ INSTRUCTIONS BEFORE COMPLETING FORM |
|---|---|
| 1. REPORT NUMBER: TR No. 38 | 2. GOVT ACCESSION NO: AD-A086 335 |
| 3. RECIPIENT'S CATALOG NUMBER: TR 38 |
| 4. TITLE (and Subtitle): Influence of Small Scale Yielding on Dynamic Fracture. | 5. TYPE OF REPORT & PERIOD COVERED: Interim Report. |
| 6. PERFORMING ORG. REPORT NUMBER: 38 |
| 7. AUTHOR(s): A.S. Kobayashi, M. Ramulu and B.S-J Kang | 8. CONTRACT OR GRANT NUMBER(s): N00014-76-C-0060 NR 064-478 |
| 9. PERFORMING ORGANIZATION NAME AND ADDRESS: University of Washington, Department of Mechanical Engineering, Seattle, Washington 98195 | 10. PROGRAM ELEMENT, PROJECT, TASK AREA & WORK UNIT NUMBERS |
| 11. CONTROLLING OFFICE NAME AND ADDRESS: Office of Naval Research, Arlington, Virginia | 12. REPORT DATE: May 1980 |
| | 13. NUMBER OF PAGES: 17 |
| 14. MONITORING AGENCY NAME & ADDRESS (if different from Controlling Office) | 15. SECURITY CLASS. (of this report): Unclassified |
| | 15a. DECLASSIFICATION/DOWNGRADING SCHEDULE |

16. DISTRIBUTION STATEMENT (of this Report)

Unlimited

14 TR-38

DISTRIBUTION STATEMENT A
Approved for public release;
Distribution unlimited

17. DISTRIBUTION STATEMENT (of the abstract entered in Block 20, if different from Report)

12 21

18. SUPPLEMENTARY NOTES

19. KEY WORDS (Continue on reverse side if necessary and identify by block number)

Fracture Mechanics
Crack Propagation
Crack Arrest
Fracture Dynamics
Dynamic Photoelasticity
Dynamic Finite Element Analysis

20. ABSTRACT (Continue on reverse side if necessary and identify by block number)

Dynamic fracture and crack-arrest responses of the well-discussed wedge-loaded rectangular, double cantilever beam (WL-RDCB) specimens machined from a 3.2 mm thick annealed polycarbonate sheet were studied by dynamic photoelasticity and dynamic finite element analysis. A small, but finite plastic yield zone surrounded the propagating crack which resulted in crack velocities, dynamic fracture toughness and crack arrest toughness lower than those observed previously in 6.4 mm thick polycarbonate fracture specimens.

DD FORM 1 JAN 73 1473 EDITION OF 1 NOV 65 IS OBSOLETE
S/N 0102-014-6601

UNCLASSIFIED
SECURITY CLASSIFICATION OF THIS PAGE (When Data Entered)

400344